

5.5 The Feynman rules of QFD

Now we have learned already a lot about the Lagrange density of QFD. To obtain the Feynman rules we can start from L_{QFD} in the unitary gauge, see eq. (5.76), which tells us immediately about the particle content of the theory. These Feynman rules in the unitary gauge are listed below.

satisfy the condition

$$(\mathbf{W}_\mu^-)^\dagger = \mathbf{W}_\mu^+. \quad (\text{G.16})$$

The expansion of \mathbf{W}_μ^- reads

$$\mathbf{W}_\mu^-(x) = \int \frac{d^3k}{(2\pi)^3 2\omega} \sum_{j=1}^3 \{e^{ikx} \epsilon_{j\mu}^*(k) \mathbf{b}_j^\dagger(k) + e^{-ikx} \epsilon_{j\mu}(k) \mathbf{a}_j(k)\}, \quad (\text{G.17})$$

where we now have $k^0 = \omega \equiv +\sqrt{m_W^2 + \mathbf{k}^2}$. Furthermore, the annihilation operators $\mathbf{a}_j(k)$ and $\mathbf{b}_j(k)$ of W^- and W^+ particles satisfy the commutation rules:

$$[\mathbf{a}_i(k), \mathbf{a}_j^\dagger(k')] = [\mathbf{b}_i(k), \mathbf{b}_j^\dagger(k')] = \delta_{ij} (2\pi)^3 2\omega \delta^3(\mathbf{k} - \mathbf{k}'). \quad (\text{G.18})$$

The starting point for a derivation of the Feynman rules for the standard model in the unitary gauge is the Lagrange density of (22.123). In order to obtain the desired rules one can apply either the canonical formalism (see Weinberg 1973) or the path-integral method (see, e.g., Itzykson 1980). Here we will simply give the result.

The rules for incoming, outgoing, and virtual fermions, photons, and gluons remain the same as in QED and QCD (Appendices B and D). It should be noted, however, that in the standard model only left-handed neutrino fields appear. This means that only u_- occurs as Dirac spinor in the wave function of an external neutrino, and only v_- for antineutrinos (21.20), (21.21).

All vertices and rules concerning gluons remain as in QCD.

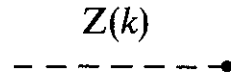
The following rules—specific to QFD—represent the additions.

<p>W^- initial state</p> <p>$\epsilon(k)$</p>	<p>incoming W line</p> <p style="text-align: center;">$W^-(k)$</p> <p style="text-align: center;">-----▶-----</p>
<p>W^- in final state</p> <p>$\epsilon^*(k)$</p>	<p>outgoing W line</p> <p style="text-align: center;">$W^-(k)$</p> <p style="text-align: center;">◀-----</p>
<p>W^+ in initial state</p> <p>$\epsilon(k)$</p>	<p>outgoing W line</p> <p style="text-align: center;">$W^+(k)$</p> <p style="text-align: center;">◀-----</p>
<p>W^+ in final state</p> <p>$\epsilon^*(k)$</p>	<p>incoming W line</p> <p style="text-align: center;">$W^+(k)$</p> <p style="text-align: center;">-----▶-----</p>

Z in initial (final) state

$$\varepsilon(k)(\varepsilon^*(k))$$

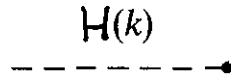
external Z line



Higgs particle in initial (final) state

$$1$$

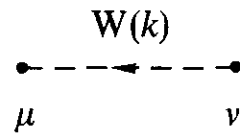
external H line



virtual W boson

$$\frac{i \left(-g^{\mu\nu} + \frac{k^\mu k^\nu}{m_W^2} \right)}{k^2 - m_W^2 + i\epsilon}$$

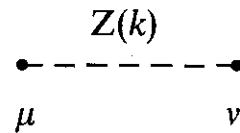
internal W line



virtual Z boson

$$\frac{i \left(-g^{\mu\nu} + \frac{k^\mu k^\nu}{m_Z^2} \right)}{k^2 - m_Z^2 + i\epsilon}$$

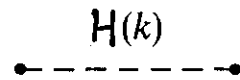
internal Z line



virtual Higgs particle

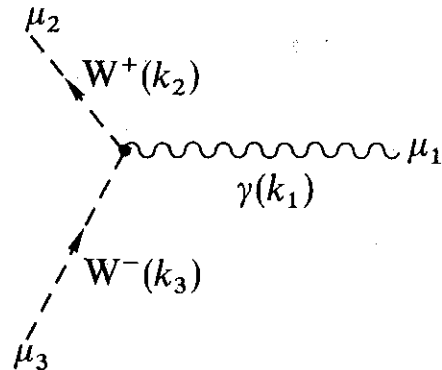
$$\frac{i}{k^2 - m^2 + i\epsilon}$$

internal H line

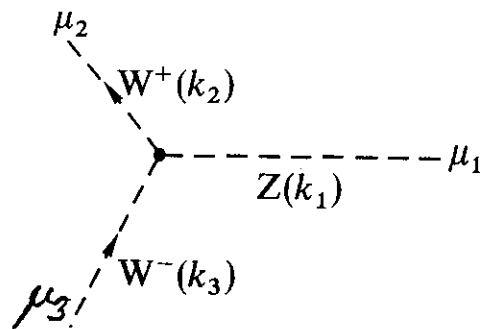


Vertices with 3 vector bosons $\left(\sum_{j=1}^3 k_j = 0, \text{ all momenta incoming} \right)$:

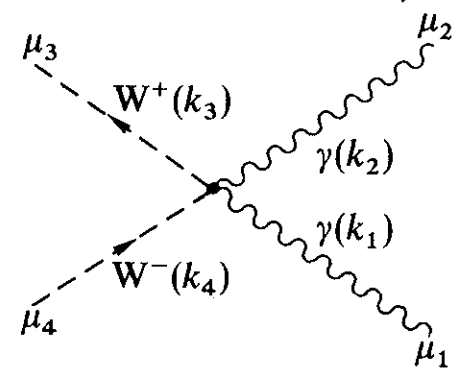
$$ie \{ (k_1 - k_2)_{\mu_3} g_{\mu_1 \mu_2} + (k_2 - k_3)_{\mu_1} g_{\mu_2 \mu_3} + (k_3 - k_1)_{\mu_2} g_{\mu_3 \mu_1} \}$$



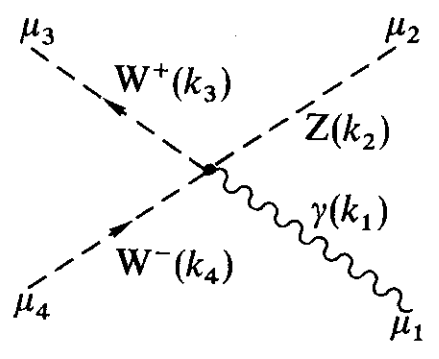
$$ie \frac{\cos \vartheta_W}{\sin \vartheta_W} \{ \text{as above} \}$$



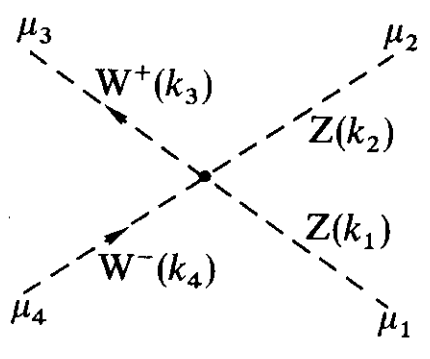
$$ie^2 \{ g_{\mu_1 \mu_3} g_{\mu_2 \mu_4} + g_{\mu_1 \mu_4} g_{\mu_2 \mu_3} - 2g_{\mu_1 \mu_2} g_{\mu_3 \mu_4} \}$$



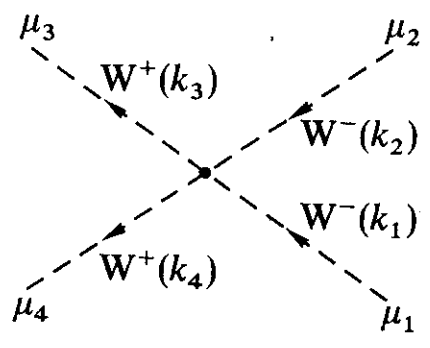
$$ie^2 \frac{\cos \vartheta_W}{\sin \vartheta_W} \{ \text{as above} \}$$



$$ie^2 \frac{\cos^2 \vartheta_W}{\sin^2 \vartheta_W} \{ \text{as above} \}$$

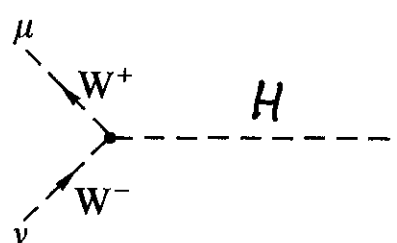


$$-ie^2 \frac{1}{\sin^2 \vartheta_W} \{ \text{as above} \}$$

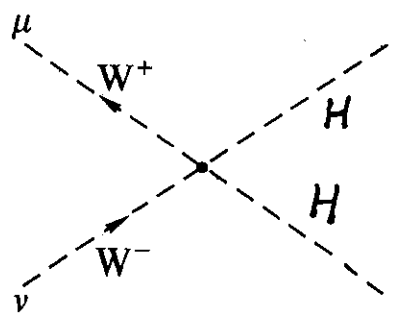


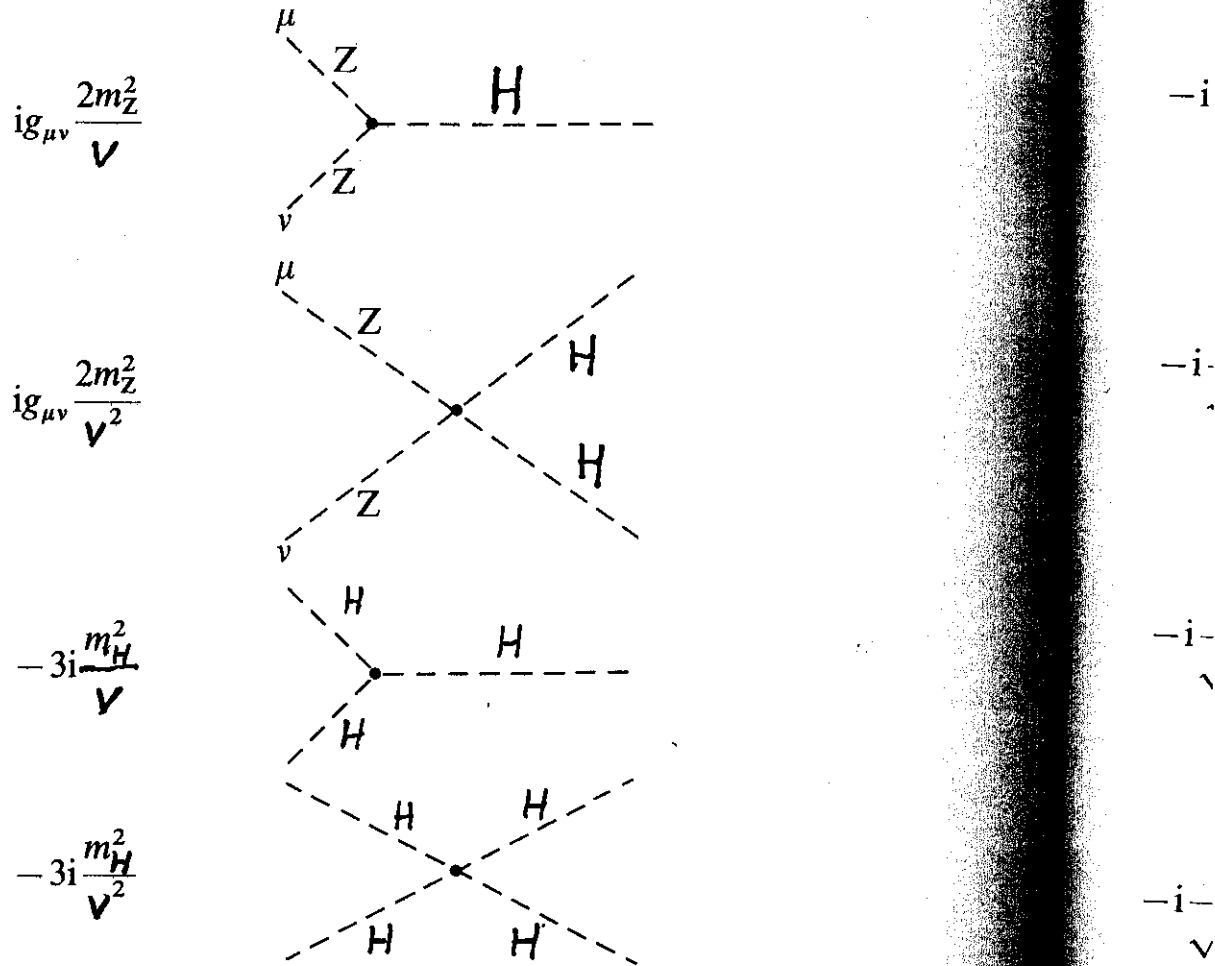
Vertices with Higgs bosons:

$$ig_{\mu\nu} \frac{2m_W^2}{v}$$



$$ig_{\mu\nu} \frac{2m_W^2}{v^2}$$





In the following we will number the leptons and quarks of the various families according to the scheme:

$$\begin{aligned}
 \nu_1 &\equiv \nu_e, & \nu_2 &\equiv \nu_\mu, & \nu_3 &\equiv \nu_\tau; \\
 \ell_1 &\equiv e, & \ell_2 &\equiv \mu, & \ell_3 &\equiv \tau; \\
 u_1 &\equiv u, & u_2 &\equiv c, & u_3 &\equiv t; \\
 d_1 &\equiv d, & d_2 &\equiv s, & d_3 &\equiv b.
 \end{aligned}$$

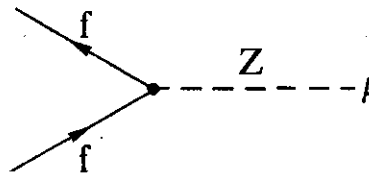
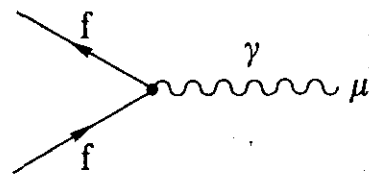
$$-i \frac{m_l}{\rho_c}$$

To refer to an arbitrary one of these particles we will use the generic label f ; the electric charge is then Q_f , and T_3^f is the eigenvalue obtained by applying the third component of the weak isospin to the *left-handed* part of f . From (22.123), (22.77), (22.112)–(22.114), we then obtain the following vertices:

Fermion–Boson vertices:

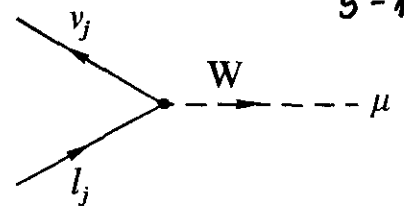
$$-ieQ_f \gamma^\mu$$

$$-i \frac{e}{\sin \vartheta_w \cos \vartheta_w} \left\{ T_3^f \gamma^\mu \frac{1 - \gamma_5}{2} - \sin^2 \vartheta_w Q_f \gamma^\mu \right\}$$

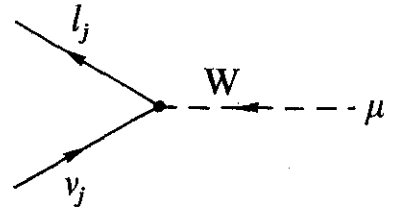


Wi mode gauge ρ' , or calcul suited highly shows out su diagra e.g., th

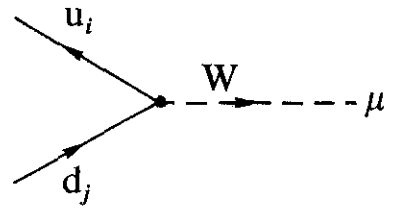
$$-i \frac{e}{\sqrt{2} \sin \vartheta_W} \gamma^\mu \frac{1 - \gamma_5}{2}$$



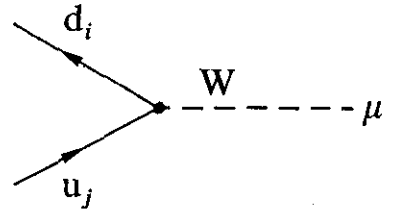
$$-i \frac{e}{\sqrt{2} \sin \vartheta_W} \gamma^\mu \frac{1 - \gamma_5}{2}$$



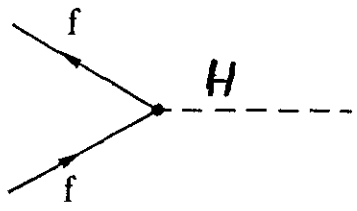
$$-i \frac{e}{\sqrt{2} \sin \vartheta_W} V_{ij} \gamma^\mu \frac{1 - \gamma_5}{2}$$



$$-i \frac{e}{\sqrt{2} \sin \vartheta_W} V_{ji}^* \gamma^\mu \frac{1 - \gamma_5}{2}$$



$$-i \frac{m_f}{V}$$



With the aid of these rules one can calculate all tree diagrams in the standard model. For diagrams that include loops one must—even in the unitary gauge—also consider Fadeev–Popov ghosts, which couple to the Higgs field ρ' , or corresponding contact terms (see Weinberg 1973). However, for the calculation of diagrams with loops, the unitary gauge is not particularly well suited since its individual diagrams—as in a *nonrenormalizable* theory—are highly divergent, although the sum of the diagrams of a particular order shows only the divergence of a *renormalizable* theory. Thus for carrying out such calculations, one usually chooses a gauge in which the individual diagrams themselves only possess the divergences of a renormalizable theory, e.g., the Feynman–'t Hooft gauge (see, e.g., Itzkyson 1980; Becher 1984).

ous

lf;
ing
om

, μ

-μ



For higher order calculations involving loops the unitary gauge is not convenient. Instead, one has to use so called renormalisable gauges like the Feynman-'t Hooft gauge. There "unphysical particles" as well as "Faddeev Popov ghosts" have to be considered, complicating the calculations.

6 Higgs Physics

We have seen in chapter 5 that the Higgs field plays a central role in QFD. In this chapter we shall outline the profile of the physical Higgs particle as it is predicted by the SM.

We discuss first the mass of the Higgs particle which is given as

$$m_H^2 = 2\lambda v^2, \quad (6.1)$$

see eq. (5.70). Here $v \approx 246 \text{ GeV}$ is the Higgs vacuum expectation value

✓

and λ is the quartic Higgs coupling constant. Typically, we would prefer λ to be small, $\lambda < 1$ say. Otherwise the self coupling in the Higgs sector becomes so large that the Lagrange density, eq. (5.76), is no longer a good guide to read off the particle content and properties of the Higgs sector.

For strongly interacting Higgs fields resonances may form, we may have a whole spectrum of bound states which somehow could, together, play the role of the Higgs particle etc.

Thus, requiring $\lambda < 1$, we have a first theoretical prejudice for a Higgs mass:

$$m_H < \sqrt{2} v \cong 350 \text{ GeV.}$$

(6.2)

There are also more serious arguments which use the renormalisation group and the triviality of the pure φ^4 theory. From these arguments one finds that for a small Higgs mass the SM is viable up to very high energy scales, for Higgses of higher mass only up to smaller

✓

energy scales. An upper bound

$$m_H \lesssim 700 \text{ GeV} \quad (6.3)$$

results from this. At the upper bound the new physics must set in at the Higgs mass scale itself.

✓

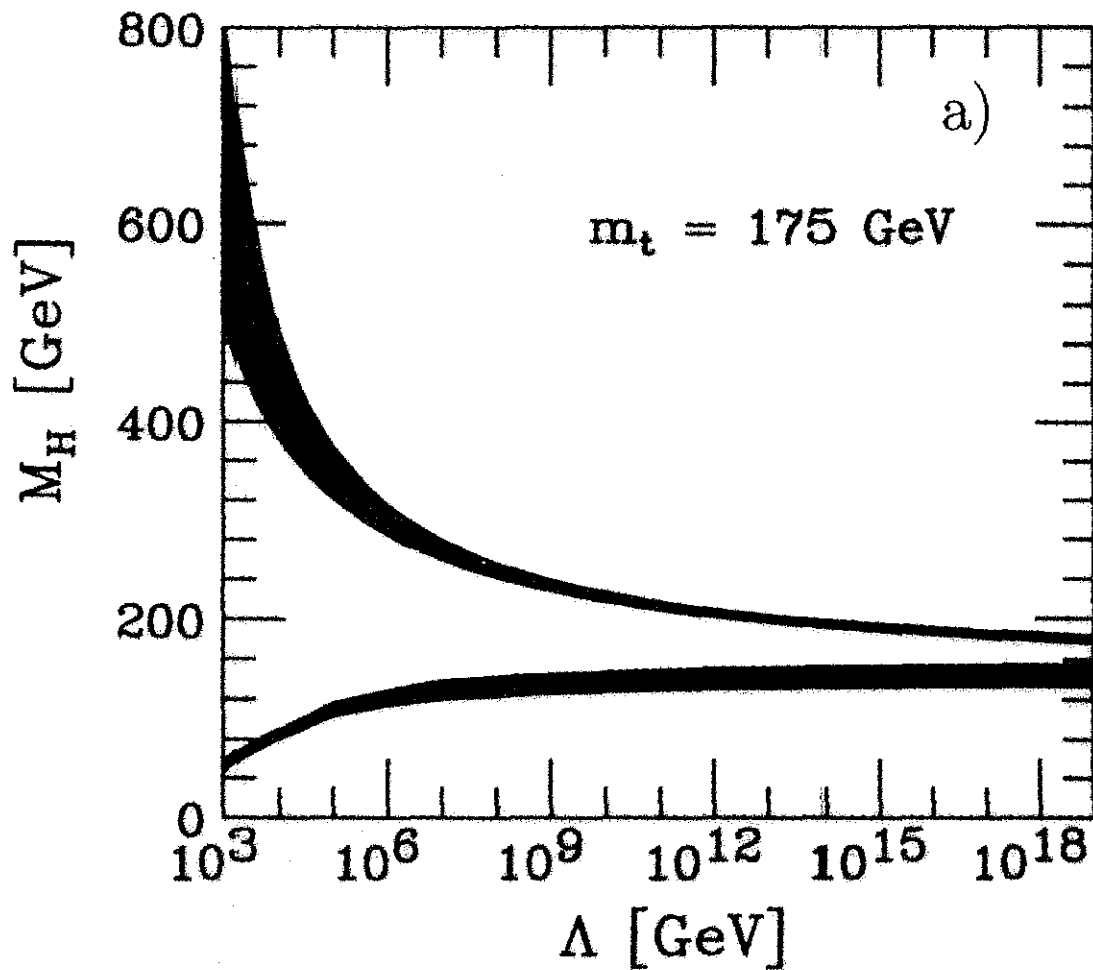


Fig. 6.1 Upper and lower bounds for the Higgs mass in the SM as function of the scale of "new physics" Λ .

(From TESLA Tech. Design Report, 2001)

In more detail, the upper bound for the Higgs mass as function of Λ results from the following considerations. As all coupling parameters in QFT the coupling parameter describing the quartic self coupling of the Higgs particles should be considered as an effective, scale dependent parameter:

$$\lambda = \lambda(M). \quad (6.3a)$$

Here M is the renormalisation scale.

Now one can calculate this dependence

of λ on M . This has been done using ^{perturbation theory} but also using $\sqrt{\text{non-perturbative}}$ techniques, ✓

for instance lattice calculations.

It is found that $\lambda(M)$

increases with M . The $\lambda\phi^4$

theory is not asymptotically free.

If we start with a certain value

for $\lambda_0 \equiv \lambda(M_0)$ at $M_0 = 100 \text{ GeV}$

say we find that $\lambda(M)$

diverges at some ^{higher} value $M = \Lambda$.
which depends on λ_0 .

This disaster happens at

higher and higher Λ the

smaller and smaller λ_0 is.

If we require the theory to

make sense up to $\Lambda = \infty$

we find that only $\lambda_0 = 0$ is

the possible starting point. ✓

Only the trivial, the non interacting, scalar theory is viable up to $\Lambda = \infty$. This is often referred to as the "triviality of the ϕ^4 theory".


The above considerations lead, via $m_H^2 = 2\lambda v^2$ to the upper bound on m_H as function of Λ in fig. 6.1.

The lower bound on m_H as function of λ in fig. 6.1 results from considerations of vacuum stability. In higher orders the Higgs potential $V(\phi)$ gets also corrections, for instance ✓

6-5d

from virtual $t\bar{t}$ pairs in
the vacuum. This gives a
negative correction to λ .

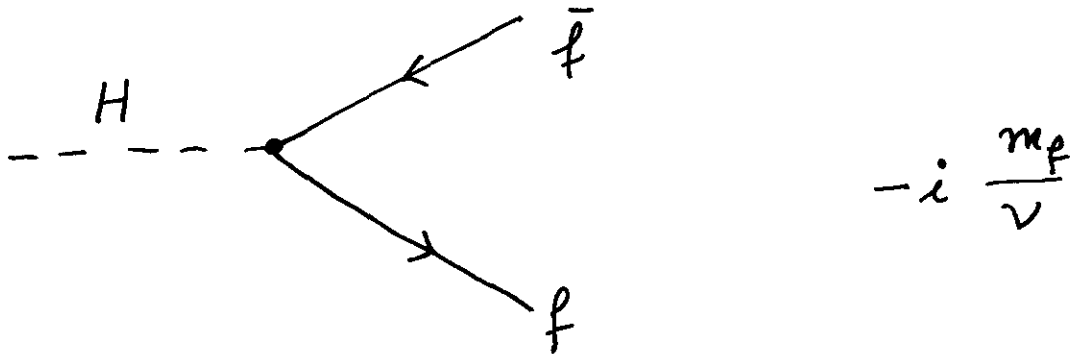
If the Higgs mass, and thus
 λ , is too small these negative
corrections lead to an unstable
potential.



Let us next turn to the decay modes of the SM-Higgs particle. We have emphasised in chapter 5 that the Higgs field provides mass to the W and Z bosons and to the fermions. As a consequence we find that the gauge-boson Higgs couplings are proportional to m_W^2 and m_Z^2 , respectively. The fermion-Higgs couplings are proportional to m_f . Using the Feynman rules of QFD, given in section 5.5, we can easily calculate the decay rates for the processes which are allowed at tree diagram level.

✓

Higgs decays to fermion - antifermion



The decay

$$H \rightarrow f \bar{f}$$

is possible for $m_H > 2m_f$.

Its decay rate is

$$\Gamma(H \rightarrow f \bar{f}) = \frac{m_H}{8\pi} \left(\frac{m_f}{v}\right)^2 N_c^f \left(1 - \frac{4m_f^2}{m_H^2}\right)^{3/2}$$

$$N_c^f = 1 \quad \text{for } f = \text{lepton,}$$

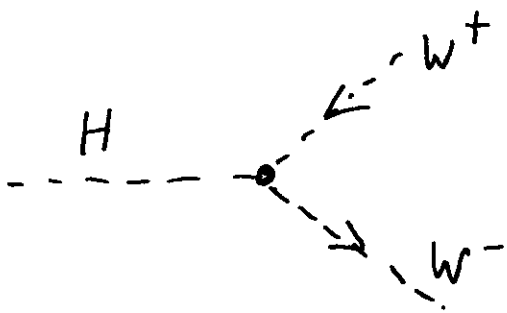
$$N_c^f = 3 \quad \text{for } f = \text{quark.}$$

(6.4) ✓

Higgs decay to W^+W^-

$$H \rightarrow W^+W^-$$

is possible for $m_H > 2m_W \approx 161 \text{ GeV}$.



$$i g_{\mu\nu} \frac{2m_W^2}{v}$$

$$\Gamma(H \rightarrow W^+W^-) = \frac{m_H}{16\pi} \left(\frac{m_H}{v} \right)^2$$

$$\left(1 - \frac{4m_W^2}{m_H^2} \right)^{1/2} \left(1 - 4 \frac{m_W^2}{m_H^2} + 12 \frac{m_W^4}{m_H^4} \right)$$

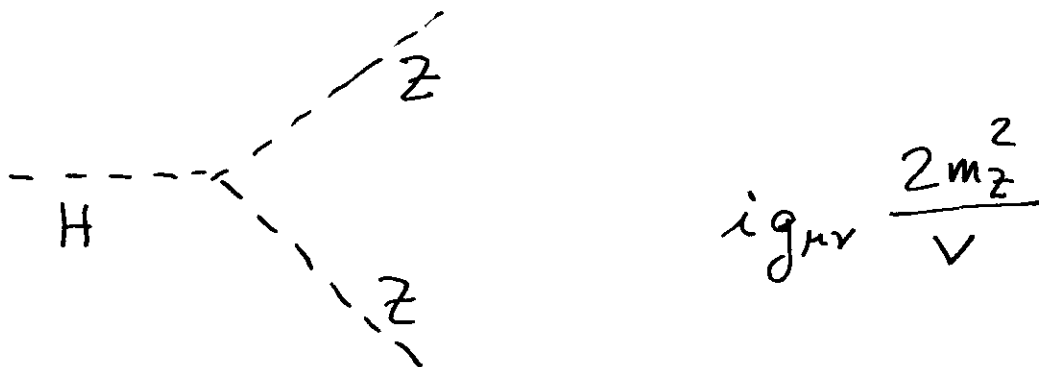
(6.5)

✓

Higgs decay to ZZ,

$$H \rightarrow ZZ$$

is possible for $m_H > 2m_Z \cong 182 \text{ GeV}$.



$$\Gamma(H \rightarrow ZZ) = \frac{m_H}{32\pi} \left(\frac{m_H}{v} \right)^2$$

$$\left(1 - \frac{4m_Z^2}{m_H^2} \right)^{1/2} \left(1 - 4 \frac{m_Z^2}{m_H^2} + 12 \frac{m_Z^4}{m_H^4} \right)$$

(6.6)

✓

Due to its coupling to the mass the Higgs particle will thus mostly decay into the most heavy particles to which a decay is energetically possible. For the range

$$115 \text{ GeV} < m_H < 2m_W \cong 161 \text{ GeV} \quad (6.7)$$

the main Higgs decay mode is

$$H \rightarrow b \bar{b}. \quad (6.8)$$

For

$$m_H > 2m_W \cong 161 \text{ GeV} \quad (6.9)$$

the decay $H \rightarrow W^+W^-$ takes over as main mode and this stays

so up to $m_H = 700 \text{ GeV}$, see fig. 6.2. ✓

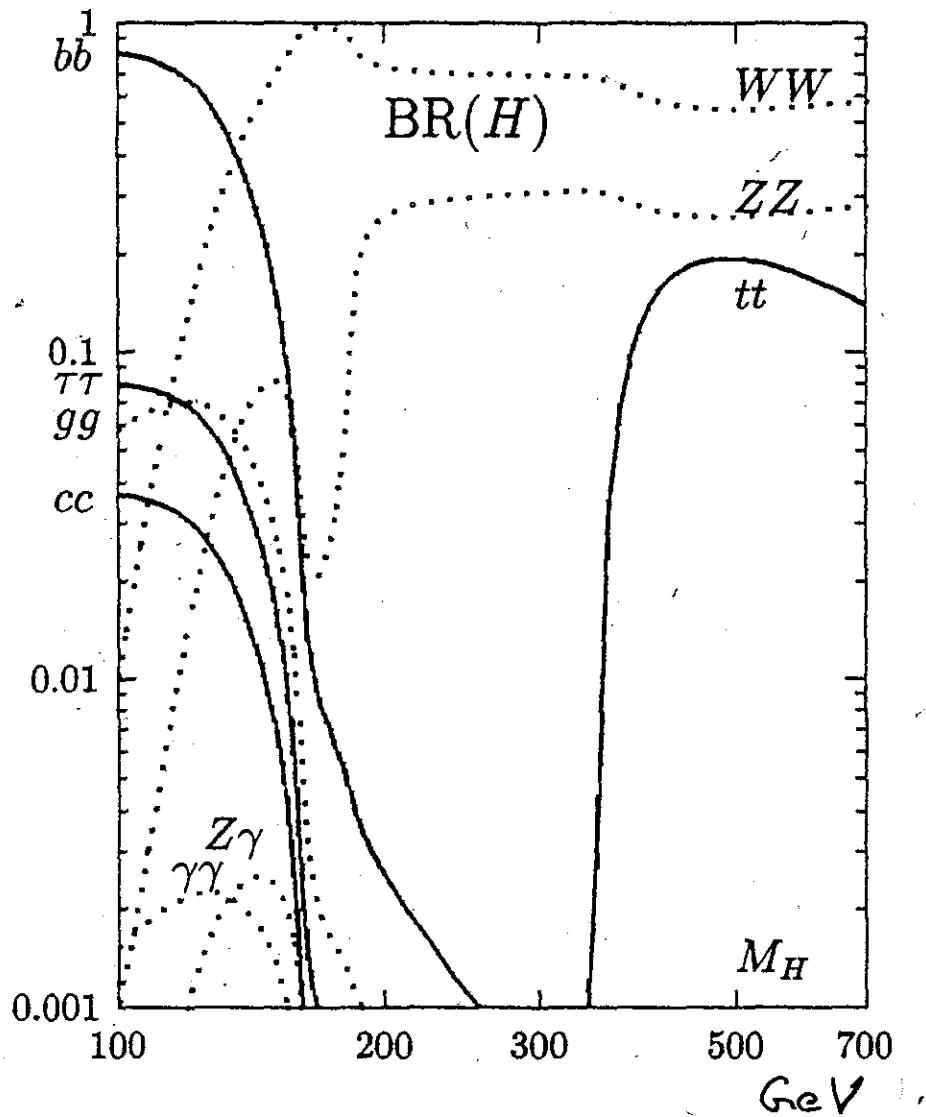


Fig. 6.2 The branching fractions of the Higgs particle in the SM as function of the Higgs mass (from TESLA TDR, 2001)

We want to draw attention to the following feature of our results for $\Gamma(H \rightarrow W^+W^-)$ and $\Gamma(H \rightarrow ZZ)$, eqs. (6.5) and (6.6), respectively. For large Higgs masses, $m_H \gg m_W, m_Z$, we find

$$\Gamma(H \rightarrow W^+W^-) \propto m_H \left(\frac{m_H}{v} \right)^2,$$

$$\Gamma(H \rightarrow ZZ) \propto m_H \left(\frac{m_H}{v} \right)^2,$$

(6.6a)

not a proportionality to $(m_W^2/v)^2$ and $(m_Z^2/v)^2$ as we would expect from the coupling parameters. Technically this is due to

✓

Thus, in

$$H \rightarrow W_L W_L$$

two powers of m_W occur
in the denominator eating up
the m_W^2 from the coupling.

The deep reason for this
is to be seen in SSB.

The longitudinal vector bosons
are, in a certain sense, the neutral
and charged partners of the physical
Higgs particle H . After SSB
we have "rotated" these
partners away in the unitary gauge.

✓

Looking at the Feynman rules of QFD we see that the trilinear Higgs coupling HHH is proportional to m_H^2/v , see p. 5-117. For a decay of a Higgs particle H to two charged scalar particles $H^+ H^-$ of the same coupling we would get

$$\Gamma(H \rightarrow H^+ H^-) \propto m_H \left(\frac{m_H}{v} \right)^2. \quad (6.6d)$$

This is precisely what we find in eq. (6.6a). At high energy the W_L^\pm and Z_L vector boson long. polarisation degrees of freedom remember their "origin" in the Higgs sector. ✓

The total width $\Gamma(H)$ of the Higgs particle is also very interesting, see fig. 6.3. For Higgs masses $m_H \cong 120 \text{ GeV}$ the total width is small, $\Gamma(H) \cong 3 \text{ MeV}$.

We can then really speak of a particle since $\Gamma(H)/m_H \ll 1$.

To be precise, the Higgs "particle" is then a very narrow resonance.

But, as we see from fig. 6.3 the total width $\Gamma(H)$ increases dramatically once the decays

$H \rightarrow W^+W^-$ and $H \rightarrow ZZ$ are energetically possible.

For $m_H \gtrsim 600 \text{ GeV}$ the total width $\Gamma(H) \gtrsim 100 \text{ GeV}$.

Thus, we are then dealing with an extremely broad resonance.

This again shows that for a heavy Higgs particle the Higgs-interactions become strong. We should then consider the perturbative results discussed above rather as an indication of what may happen than as precision predictions.

✓

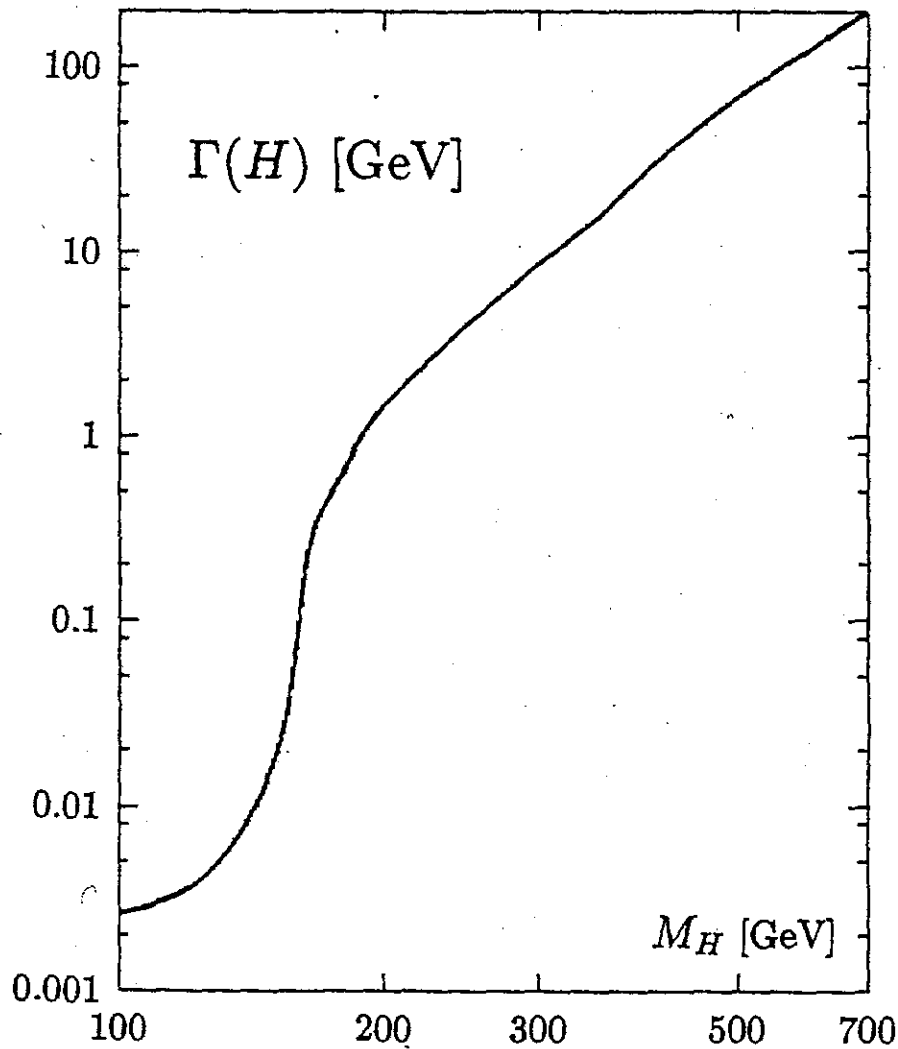


Fig. 6.3 The total width of the Higgs particle in the SM as function of the Higgs mass (from TESLA TDR, 2001)

✓

Next we want to discuss two decay channels of the Higgs particle which can only proceed via loop diagrams.

These are:

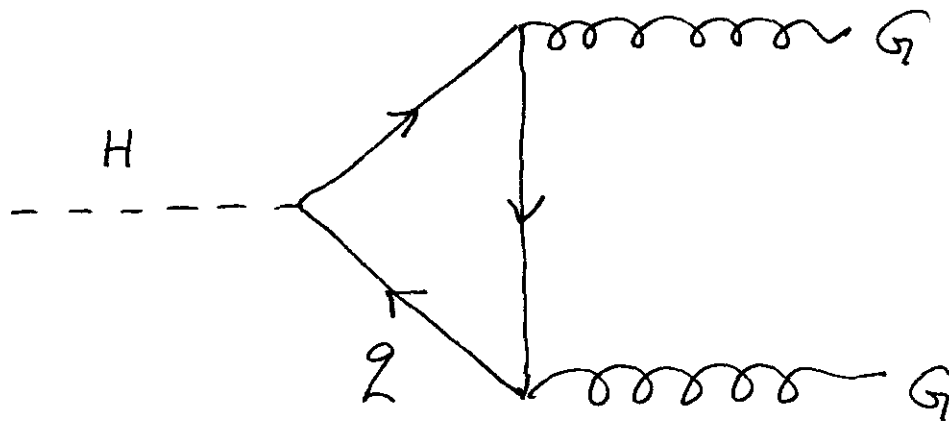
$$H \rightarrow G G, \quad (6.10)$$

$$H \rightarrow \gamma \gamma. \quad (6.12)$$

✓

6-16

The decay Higgs \rightarrow 2 gluons
can proceed via a quark loop



+ crossed diagram

In principle any quark flavour q
must be considered in this loop.
But, since the Higgs - quark
coupling is proportional to m_q ,
only the heaviest quark, the
top quark, really matters.

✓

One finds from the above diagrams

$$\Gamma(H \rightarrow GG) = \frac{m_H}{8\pi} \left(\frac{m_H}{v} \right)^2 \left(\frac{\alpha_s}{\pi} \right)^2 \left| \sum_2 \left(\frac{m_2}{m_H} \right)^2 \mathcal{J} \left(\frac{4m_2^2}{m_H^2} \right) \right|^2,$$

(6.13)

where

$$\mathcal{J}(z) = \int_0^1 dv \frac{1-v}{z-v-i\epsilon} \cdot \ln \frac{1 + \sqrt{1-v}}{1 - \sqrt{1-v}}.$$

(6.14)

For $z = 1$ we get

$$J(1) = 2. \quad (6.15)$$

For $z \rightarrow \infty$ we find

$$J(z) \rightarrow \frac{4}{3z}. \quad (6.16)$$

Thus for a light Higgs particle

$m_H \approx 120 \text{ GeV}$ we have for $q = t$

$$z = \frac{4m_t^2}{m_H^2} \approx 8.5,$$

$$\Gamma(H \rightarrow GG) \cong \frac{1}{72\pi} m_H \left(\frac{m_H}{v}\right)^2 \left(\frac{\alpha_s}{\pi}\right)^2.$$

(6.17)

Numerically, this gives for $m_H = 120 \text{ GeV}$

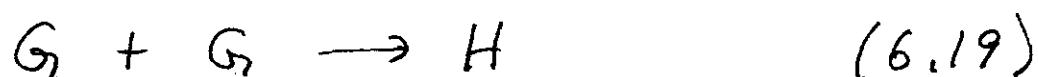
$$\text{and } \alpha_s = 0.12$$

$$\Gamma(H \rightarrow G_2 G_2) \cong 0.18 \text{ MeV},$$

$$\text{Br}(H \rightarrow G_2 G_2) \cong 6\%.$$

(6.18)

Thus, for the decays this does not give a large branching fraction. But the reverse process

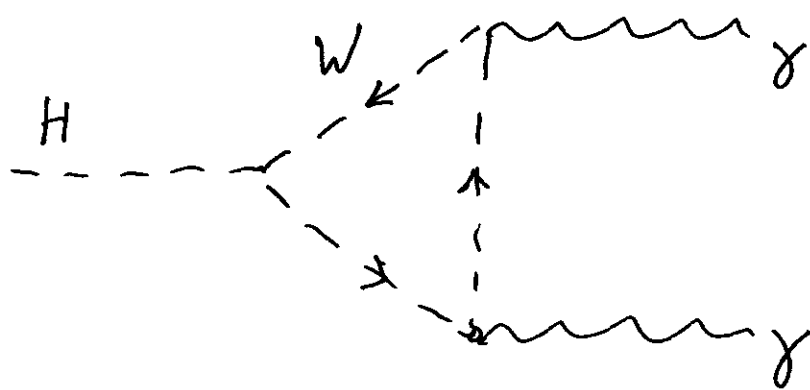
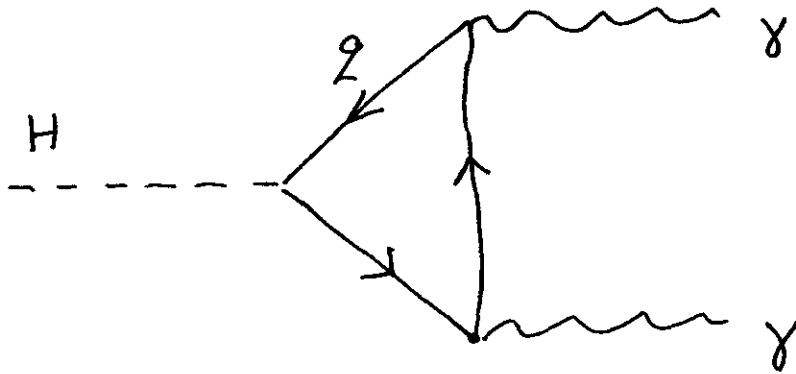


is the main production mechanism of a SM Higgs particle at the LHC as we shall discuss below.

The decay

$$H \rightarrow \gamma \gamma$$

proceeds, in leading order,
through the following loop diagrams



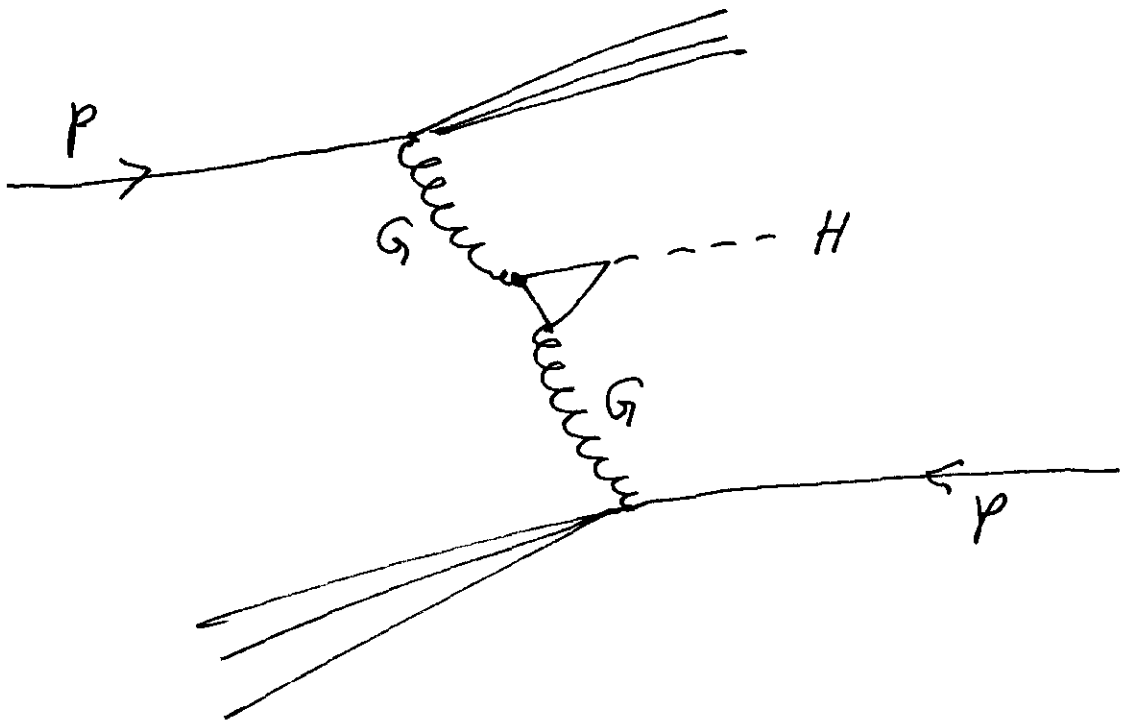
+ crossed diagrams

The branching fraction for $H \rightarrow \gamma\gamma$ is small, see fig. 6.2. For $m_H \cong 120 \text{ GeV}$ we have

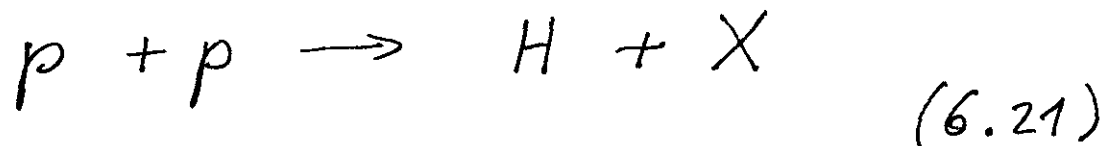
$$\text{Br}(H \rightarrow \gamma\gamma) \cong 2\% \quad (6.20)$$

Nevertheless, this decay channel is very important. It offers the best chance to discover a light Higgs particle, $m_H \cong 120 \text{ GeV}$, at the LHC.

Finally, we say some words on the production mechanisms for the SM Higgs particle at the LHC. The main production mechanism is expected to be gluon-gluon fusion, eq. (6.19).



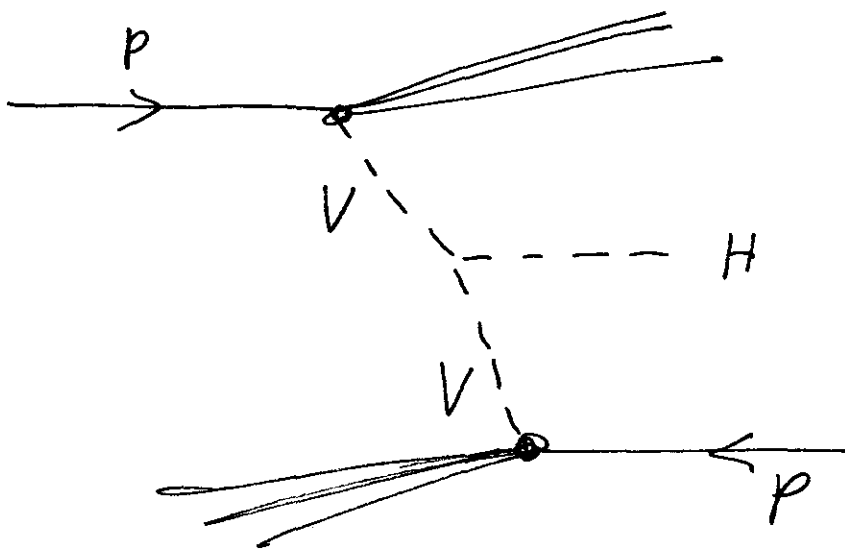
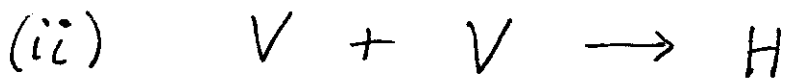
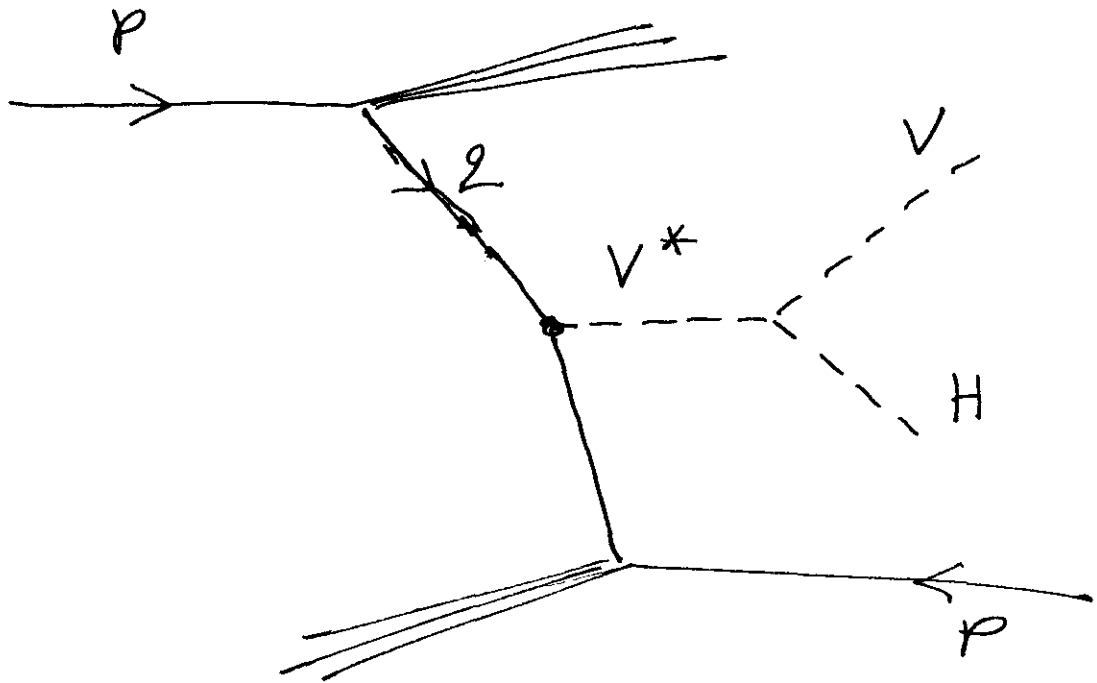
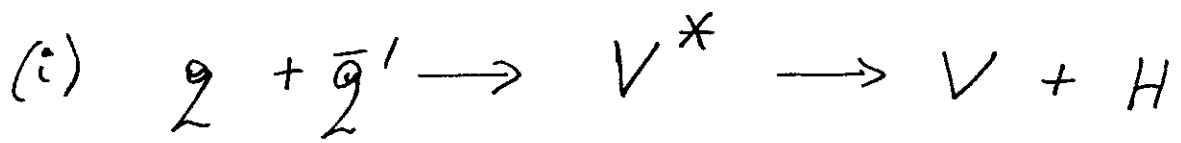
The rate for this reaction

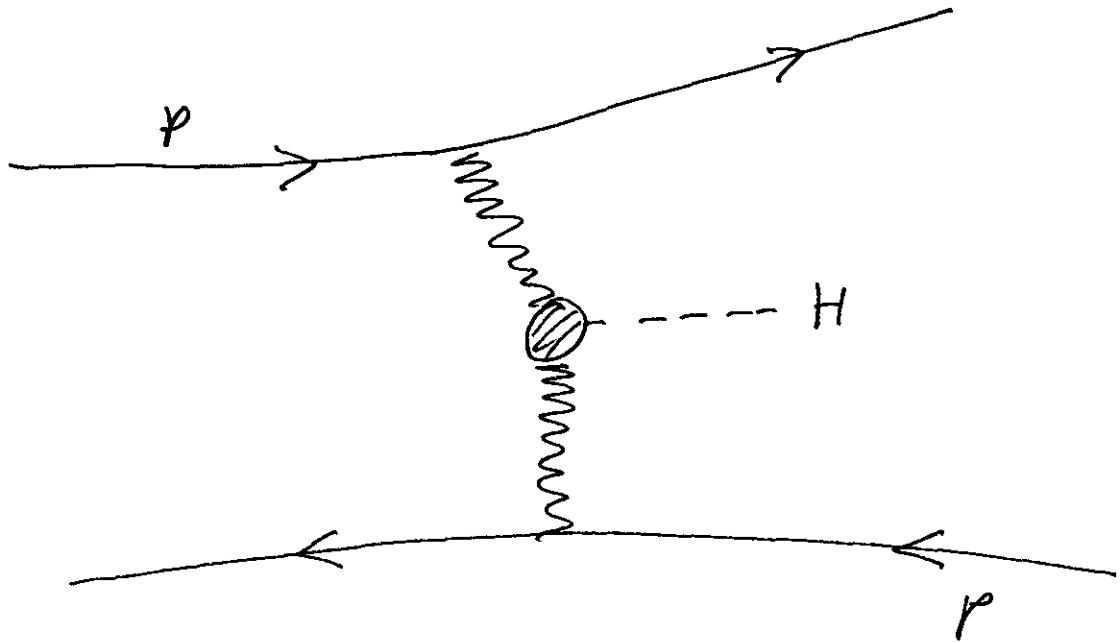


can be calculated using the result for $\Gamma(H \rightarrow GG)$ and the gluon distributions of the proton. The latter are obtained from the HERA results.

Other production mechanisms are via production of a single virtual vector boson, via vector boson fusion and in diffractive collisions.

In the following $V = W$ and Z .





At gluon level, the simplest diagram is as follows

